February 1986

NOTICE

This report contains information of a preliminary nature and was prepared primarily for internal use at the originating installation. It is subject to revision or correction and therefore does not represent a final report. It is passed to the recipient in confidence and should not be abstracted or further disclosed without the approval of the originating installation or USDOE Office of Scientific and Technical Information, Oak Ridge, TN 37830.

ANL-IFR--36

TI86 025969

COMPATIBILITY OF U-Pu-Zr FUELS WITH ADVANCED CLAD ALLOYS: ONSET-OF-MELTING RESULTS

by

A. G. Hins

Materials Science and Technology Division
Argonne National Laboratory
9700 South Cass Avenue
Argonne, Illinois 60439

APPLIED TECHNOLOGY

Any Further Distribution by any Holder of this Document or of the Data Therein to Third Parties Representing Foreign Interests, Foreign Governments, Foreign Companies and Foreign Subsidiaries or Foreign Divisions of U S Companies Should Be Coordinated with the Deputy Assistant Secretary for Reactor Systems, Development and Technology, Department of Energy

IFR TECHNICAL MEMORANDUM NO. 36

Results reported in the IFR-TM series of memoranda frequently are preliminary and subject to revision. Consequently they should not be quoted or referenced without the author's permission.

Reviewed by David Hamrin and determined to be Unlimited Release 05/17/2019

APPLIED TECHNOLOGY

Any further distribution by any holder of this document or of the data therein to third parties representing foreign interests, foreign governments, foreign companies and foreign subsidiaries or foreign divisions of U. S. companies should be coordinated with the Deputy Assistant Secretary for Breeder Reactor Programs, U. S. Department of Energy.

MASTER

DISCLAIMER

Released for announcement in ATF. Distribution limited to participants in the LMFBR program. Others request from RSBT, DOE.

TABLE OF CONTENTS

LIST OF FIGURES

LIST OF TABLES

COMPATIBILITY OF U-Pu-Zr FUELS WITH ADVANCED CLAD ALLOYS: ONSET-OF-MELTING RESULTS

by

A. G. Hins

ABSTRACT

U-Pu-Zr fuels are known to be compatible with stainless steel clads to an upper temperature limit that is constrained by constituent diffusion. At this thermal point the mass transfer of the constituents across the fuel/clad interface creates multicomponent phases that effect liquation, also known as onset-of-melting. Determination of the onset-of-melting temperatures for a number of fuel/clad combinations of interest to the Integral Fast Reactor (IFR) program was the goal of the initial phase of the compatibility work. Fuel/clad compatibility test couples were used to conduct the experiments. Comparisons were made between the present experimental results and the published melting-test results on EBR-II fuel/clad couples and on couples of clad alloys with early U-Pu-Zr fuels. Current experimental results indicate that the IFR advanced fuel/clad couples of primary interest exhibit higher onset-of-melting temperatures than those measured for the fuel/clad combination currently in operation in EBR-II. No unexpected or restrictive chemical interactions between the IFR U-Pu-Zr fuels and advanced clad alloys were found within the temperature range of the tests.

I. INTRODUCTION

Fuel and clad chemical interactions (FCCI) in the nuclear reactor core during operation are of primary concern to the Integral Fast Reactor (IFR) program. FCCI[a] during irradiation are normally thought of as contributing a clad wastage component to the extent that the clad properties are reduced commensurately with a smaller effective clad thickness. This decrease in wall thickness reduces the load that the clad can sustain, thereby shortening life or decreasing safety margins. Reactor core designers desire fuel/clad

[a]Denotes fuel/clad chemical interactions.

combinations that will provide adequate clad performance with safety to the end-of-design life, including the wastage factor.

Previous compatibility studies have found that FCCI generally manifest a solid-state interdiffusion of fuel and clad constituents. Iron and nickel were found to migrate from the austenitic stainless steel clad into the fuel. In ferritic stainless steels, as well as in austenitic stainless steels, carbon and other interstitials are also expected to diffuse into the fuel. The resultant mechanical properties in the clad diffusion band may be degraded and, consequently, that portion of the clad wall is considered lost.

With sufficient time at higher temperatures, solid-state interdiffusion between the fuel and clad generates an interaction zone in the fuel/clad interface. Constituent mass transfer into the interaction zone creates multicomponent phases, where increasing amounts of elements such as Ni and Fe depress the solidus temperatures of U and Pu. Eutectic-type formation[a] (onset-of-melting) temperatures have been found in the past to range from 705°C in the case of U-5Fs fuel/austenitic stainless steel clad to 825°C in the case of U-15Pu-11Zr fuel/Type 316 stainless steel clad.

A high fuel/clad incipient-melting temperature provides a safety margin for off-normal events. In-reactor tests with U-5Fs fuel have shown that temperatures considerably above the incipient-melting temperature are required to achieve unsafe rates of interaction zone growth. However, unchecked onset-of-melting can be expected to ultimately lead to significant clad penetration by way of stress rupture.

This report focuses on the high-temperature compatibility studies that pertain to the onset-of-melting evaluations. Compatibility tests have been run on advanced ferritic and austenitic stainless steel clad alloys in combination with U-Pu-Zr fuels. Clad alloys of particular interest at this time are the ferritic alloys HT-9 (12Cr-1Mo) and T91 (9Cr-1Mo) and the austenitic alloy D9 (Ti-modified Type 316 stainless steel). The test fuels contained up to 19 wt.% Pu. Future tests will include Pu concentrations up to 26 wt.%.

The tests have been structured to expose any evidence of unexpected or catastrophic low-temperature eutectic formation in the particular fuel/clad

---

[a]This refers to interactions that occur in non-equilibrium states, which are differentiated from the classical binary eutectic formation reaction that occurs under equilibrium conditions.

combinations of interest to the IFR program. Current results are compared with previous findings of incipient-melting temperatures on similar fuel alloys. A future report will address in detail the related, lower temperature, diffusion band measurement experiments.

II. EXPERIMENTAL PROCEDURE

A. Test Materials

Table I lists the chemical compositions of four advanced clad alloys and three U-Pu-Zr fuel lots used in the current compatibility experiments. For comparison purposes, some tests on Type 304 stainless steel were included. The chemical composition of this material is as follows (in wt.%):[a] Cr, 18.24; Ni, 9.49; Mo, 0.27; Cu, 0.21; Mn, 1.26; Si, 0.46; P, 0.030; S, 0.006; N, 0.0315; and C, 0.06. Minor-impurities analyses for the two EFL fuel heats, which were produced at ANL-West, have not been published and will be reported later. Oxygen, carbon, and nitrogen contents in the fuel will be determined, because these interstitials are thought to have a major influence on clad/fuel diffusion dynamics. Fuel isotopic compositions are given in Table II.

Clad segments of proper length are rough cut as needed by use of a Buehler Isomet cutoff saw. Fuel test sections are cut at medium speed, also on an Isomet saw. The clad materials are stored in stock form in labeled envelopes. Fuel materials are stored in plutonium laboratory gloveboxes in similar fashion.

B. Specimen Preparation

Fuel and clad test specimens are sawcut to thicknesses of ~0.110 in. Specimen circumferential surfaces are retained in the as-received condition. The diameters are as follows (in inches): 304 SS, 0.170; 316 SS, 0.175; D9, 0.176; HT-9, 0.177; T91, 0.179; R450, 0.163; EFL029, 0.170; and EFL036, 0.170. Flat cross-sectional surfaces are hand-ground on 30-μm aluminum oxide paper to obtain parallelism. Surface flatness is especially important for generation of reliable compatibility test data. Under the constraint of glovebox operations, preparation of U-Pu-Zr fuel specimens with flat surfaces met with continued difficulty until a specimen holder was devised as a modi-

[a]Overcheck analyses done by Kawin Company on October 30, 1985.

Table I. Fuel and Clad Compositions[a]

	Material/Heat						
	U-8Pu-10Zr/ EFL029	U-15Pu-11Zr/ R450	U-19Pu-10Zr/ EFL036	HT9/ 91353 (Ferritic)	T91/ 10148 (Ferritic)	316/ 10211[b] (Aus.)	D9 83510 (Aus.)
Fe		200 ppm		Bal.	Bal.	Bal.	Bal.
Cr				12.02	9.24	17.94	13.45
Ni		100 ppm		0.57	0.16	11.15	15.61
Mo				1.03	0.96	2.15	1.65
Cu				0.03	0.08	0.16	<0.01
Co				0.01	0.019		<0.01
Nb					0.054		<0.01
Ti				0.002	0.002		0.32
V				0.34	0.21		<0.01
W				0.51	0.01		
Mn				0.50	0.47	1.75	2.05
Si		144/151 ppm		0.22	0.28	0.55	0.85
P				0.007	0.021	0.020	0.002
S				0.003	0.006	0.009	0.004
C		60/36 ppm		0.21	0.089	0.04	0.034
N		490 ppm		0.0037[c]	0.0383[c]	0.0612[c]	0.0051[c]
O		500 ppm		0.0058[c]	0.0016[c]	0.0075[c]	0.0062[c]
Al		50 ppm		0.016	0.002		0.005
B				<0.001	<0.001		<0.0005
Ta				<0.020			<0.010
As				<0.01	0.002		<0.005
Y		50 ppm					
Sn					0.004		
U	82.39	Bal.	71.75				
Pu	8.41	15.5/15.1[d]	19.26				
Zr	9.80	11.2/11.3[d]	10.34		<0.001		<0.010

[a] In wt.% except as noted.

[b] Type 316 stainless steel composition was determined by overcheck analyses in October 1985.

[c] As measured at the ANL-West Analytical Chemistry Laboratory. Certification values, where measured, may have been slightly different.

[d] Pu content is 15.6/15.7 wt.% by new analyses done in October 1985 and Zr content is 10.5/10.8 wt.% by new analyses done in January 1986.

Table II. Fuel Isotopic Compositions (wt.%)

Isotope	Fuel Heat		
	EFL029	R450[a]	EFL036
U-234	0.46	0.61	0.41
U-235	64.29	93.08	57.01
U-236	0.30	0.32	0.27
U-238	34.95	5.99	42.31
Pu-239	93.83	88.95	93.83
Pu-240	5.71	10.36	5.72
Pu-241	0.39	0.56	0.38
Pu-242	0.08	0.11	0.07

[a]From analyses performed in October 1985.

fication of the holder shown on page 6 of Ref. 1. This allowed precision positioning of the specimens during surface preparation.

Finished pieces are cleaned ultrasonically in acetone and then in ethyl alcohol. Just before assembly into test columns, the fuel and clad specimens are again hand-ground on 30-μm aluminum oxide paper with the aid of an alcohol wetting agent. The specimens are final-cleaned ultrasonically by immersion in an ethyl alcohol bath. Drying of the samples in plastic storage compartments in the glovebox atmosphere follows. Specimens are always handled with caution to preserve material identity.

C. Test Capsule Assembly

The specimen holder design in current use is shown in Fig. 1. In early tests, through test DC6, a Croloy (2¼Cr-1Mo) holder was used, and in test DC8 an Inconel holder was used. Functional problems that occurred with those early holder designs have been corrected in the design described here.

Molybdenum-containing holder material is used to provide high-temperature performance as well as to produce a lower coefficient of expansion relative to the expansion of the test column. Typically, the test column will expand in length 0.003 in. to 0.005 in. more than the holder cavity at temperature. Holders of three lengths are available to hold test columns of 3-12 specimens,

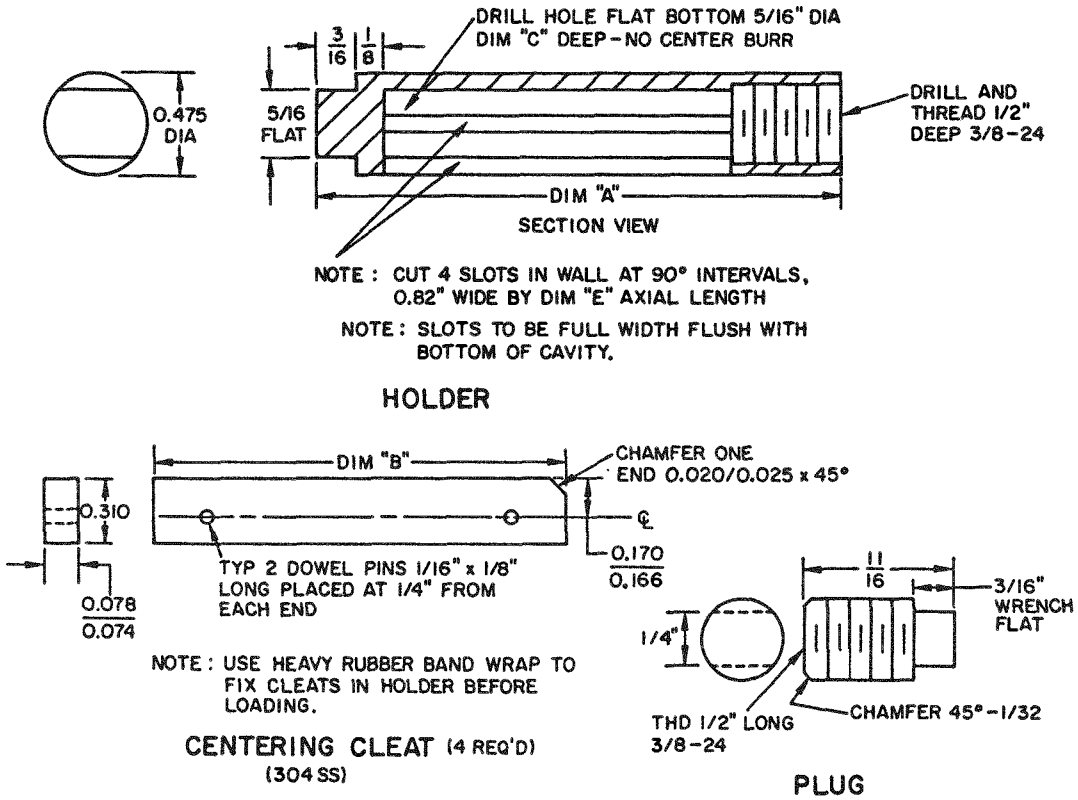

CAPSULE	DIM A	DIM B	DIM C	DIM D	DIM E
S	TBD	TBD	TBD	TBD	TBD
M	1.687	0.990	1.375	0.850	1.000
L	2.410	1.700	2.100	1.500	1.710

TYPICAL TEST COLUMN
MAX LENGTH - DIM "D"

Fig. 1. Specimen Holder for IFR Compatibility Studies.

according to the needs of the test matrix. Four centering cleats are held in place on the holder by a heavy rubber band during loading. The cleats center the test column in the holder cavity until the top plug is screwed firmly in place by use of 6-in. hand wrenches. Then the cleats are removed. The column/cavity radial gap of 0.067 in. is sufficient to prevent inadvertent contact between the test specimens and the holder wall during the heat treatment period. A radiused bearing pin applies hold-down pressure to the end of the test column without angular distortion.

Prior to assembly of a test capsule, the holder parts are ultrasonically cleaned in acetone and ethyl alcohol. Clean parts are placed in foil trays and oven-dried at 160°F overnight. Clean parts are handled with lintless cotton gloves.

Early on the day selected for test initiation, specimen holder parts are transferred to the loading glovebox. The designated fuel/clad specimens are prepared according to Section II.B of this report. Loading and assembly of the specimen holder is done in a nitrogen atmosphere glovebox, which contains approximately 0.02% oxygen, within 1 h after final specimen preparation. The finished assembly is inserted into a cleaned outer capsule made of Type 304 stainless steel. A 0.003-in.-thick zirconium foil wrap is inserted in the outer capsule to getter oxygen from the atmosphere inside the capsule. The encapsulated assembly is transferred by vinyl pouch to the welding glovebox and a GTAW weld is made to seal the final end plug onto the stainless steel capsule. Just prior to welding, the capsule volume is purged with welding-grade argon. The loading, assembly, and welding procedure is designed to be completed quickly. A maximum time lapse of 2½ h between final grinding of the test sample and initiation of the heat treatment operation is generally achieved.

D. Heat Treatment

Encapsulated compatibility test experiments are transferred into one of a bank of gloveboxed heat treatment furnaces. The furnaces were constructed in D-wing of Building 212 specifically for long-term thermal testing. Each tube furnace is water-cooled and power is supplied by a 1.5-kW saturable reactor that is controlled from a Barber Coleman model 523C digital setpoint controller. A 4-in.-long nickel heat sink inside the furnace provides thermal stabilization of the test capsule. The test temperature is monitored

from the heat sink wall and is measured by means of a Type S thermocouple, which is attached to a Fluke model 2168A multitype digital thermometer. A Wahl C-65 Thermocouple Calibration Standard Instrument is used for instrument and system calibration purposes. Heat zone overtemperature protection is provided by a Barber Coleman model 521L control unit. Long-term heat treatment test temperatures are recorded on an in-line strip chart recorder, which registers evidence of off-normal thermal conditions during unattended hours.

A control temperature variability of less than ±2°C is routinely achieved. An overall system temperature accuracy of better than ±10°C was obtained for all of the present tests. The appendix contains a summary of the test temperature calibration work.

Compatibility test runs are begun by placing the test capsule inside the nickel heat sink. The recording thermocouple is inserted into its well in the heat sink. Full power is applied to the furnace and a temperature rise rate of approximately 600°C per hour is achieved. Upon nearing the test temperature, the furnace controller is manually operated to prevent temperature "overshoot." The test run clock is started as soon as the temperature objective is reached and manual furnace control is continued within the ±2°C envelope until a stable temperature is reached. Upon completion of a heat treatment, furnace power is discontinued and the test capsule is allowed to cool in place. Cooldown rates in the range of 250-150°C per hour are achieved.

Test capsules that have completed the heat treatment are transferred to a lathe glovebox. The outer stainless steel capsule is cut away and the zirconium getter foil is inspected for evidence of air leakage or other unexpected atmosphere contaminants. The fuel/clad test column is visually examined through the slits of the specimen holder for evidence of column separation, bowing, and proper axial compression gap. Generally, the end plug cannot be unscrewed. In that case the test column is removed from the holder by cutting away a portion of the holder wall. Care is taken to prevent breakage of the brittle fuel/clad interfaces in the test column during handling.

E. Optical Metallography

The columns of fuel/clad test specimens are transferred into the metallography glovebox where each column is horizontally mounted in a 1¼-in. Koldmount self-curing resin mount. In the case of long columns or separated columns, the column may be mounted in two sections. Stainless steel collar rings and end pieces are applied to the column segments before mounting to prevent edge rounding and generally improve the polished surfaces for metallographic examination.

Test column mounts are ground on Automet mechanical polishing equipment by standard techniques. Coarse, 120-grit SiC paper is used until a minimum 0.140 in. of column width is exposed. Successive grinding steps utilize 320-, 400- and 600-grit SiC papers. All grinding is done with the aid of Hyprez lubricant. Frequent sample rotation is necessary to obtain adequate results.

Specimens are polished on the Automet wheels with Microcloth and 6-μm diamond paste in Hyprez followed by 0.05-μm alumina in distilled water. Generally, frequent repolishing is necessary during the etch-evaluation cycle, and both polishing steps are used for the repolish operation.

Although the U-Pu-Zr fuel specimens tend to atmosphere-etch over time and reveal some structure, chemical etching has been found desirable to adequately develop the fuel structures for optical evaluation. A swab etch, designated as Etchant #1, has been used exclusively for the various U-Pu-Zr alloys under test. This etchant contains 2 parts HF, 60 parts HNO_3, and 60 parts lactic acid. A short swab time of under 1 sec is typical. In some cases a 10:1 acid dilution by water is required to prevent overetching.

Ferritic clad alloys HT-9 and T91 have also responded well to Etchant #1. A swabbing period of 6 sec is typical in this case. Fuel/clad interaction band features are clearly discernible with this etchant in the cases where bands are present.

The austenitic clad alloys -- Types 304 stainless steel, 316 stainless steel, and D9 (Ti-modified 316 stainless steel) -- have required extensive electrochemical etching development to disclose the desired diffusion band and incipient-melting-zone features. Selective etching techniques are necessary to accommodate the multiple clad/fuel/clad specimen sequence in each test column under examination. A diluted Microstop lacquer liquid is

used on the fuel and ferritic clad materials with general success, when preparation is made for etching of the austenitic stainless steel specimens. However, application of the Microstop material is tedious and precise location of the liquid application is essential. The austenitic alloys are typically electroetched through a sequence of multiple steps with oxalic acid and nitric acid solutions. The two basic etchant compositions are 5% oxalic acid in distilled water and 50% nitric acid in distilled water. Typical etchant parameters are 3.6 V for 15 sec with oxalic acid and 1.5 V for 20 sec with nitric acid. The etchant sequence is continued until the desired fuel-clad interaction band features are suitably displayed for photomicrography. D9 clad alloy structures are better disclosed by electroetching with a 5% solution of chromium trioxide in water. However, the grain boundary carbide network presents a challenge for production of good-quality photomicrographs of D9 by either etchant method.

A Bausch and Lomb research metallograph is used for test couple photomicrography. The metallograph stage, along with the objective lens housing, is located inside a nitrogen atmosphere glovebox. The balance of the instrument is outside the glovebox. A 250-W, variable-power quartz-halogen lamp provides adequate illumination for the photomicrography work. Representative areas of fuel/clad interaction zones are typically photographed at 275X or 500X magnification. Dimensional measurements and other interaction band evaluations are made from the photomicrographs as well as by visual examination of specimens on the metallograph stage.

F. Scanning Electron Microscopy

Two compatibility test columns, DC4 and DC8, have been examined by scanning electron microscopy (SEM). SEM confirmation was sought for the conclusions drawn from optical metallography regarding the liquid phase formation zone of DC4. SEM analysis of DC8 was conducted to compare compositional features in typical fuel/clad diffusion zones with the incipient-melting zone of DC4. DC8 is contained in a single metallographic mount and DC4 is contained in two mounts, which are labeled DC4-1 and DC4-2. All samples are in the as-polished condition (0.05-μm alumina finish).

SEM evaluations have been conducted in the Alpha-Gamma Hot Cell Facility of Building 212 on an Etec Autoscan SEM unit. The energy-dispersive X-ray analysis mode was used. In this case, the analysis of compositions has been

qualitative and is limited primarily to the elements U, Pu, and Zr. Study of the light elements O, N, and C is not possible with SEM because of inherent instrument limitations. However, these elements will be analyzed with an Auger microprobe in the near future.

III. ONSET-OF-MELTING TEST RESULTS

A. Test Matrix

Information on onset-of-melting (incipient melting) at the fuel/clad interface has been gathered from 11 compatibility experiments. Table III lists the 11 test runs and details the specimens and interfaces present in each test. In the table, each hyphen denotes a fuel/clad interface. Generally, the tests were run serially, with results from prior tests used in part to determine succeeding test sequences. In addition, the later tests were planned to include fuel/clad combinations at all pertinent temperatures to complete the desired onset-of-melting matrix. Substantial portions of the later tests were designed to generate preliminary information on diffusion band formation, which will be featured in an upcoming report. A few U-10Zr and U-5Fs fuel samples were included in some tests to provide diffusion information for comparison with the results obtained by other workers (Refs. 2,3).

B. Early Experimental Trials

IFR requirements for compatibility testing of multiple fuel and clad materials presented the problem of testing a very large number of compatibility couples. This dictated that each thermal test vehicle contain a test column comprising 5-10 test couples. Although some U-Pu-Zr fuel compatibility tests had been run previously, as described in Ref. 4, the test vehicles and procedures were not thoroughly detailed in the available documentation. Consequently, a certain amount of trial and error development work was required to implement the early test runs described here. Test vehicles for the first five tests listed in Table III were based on the methodology described in Refs. 2 and 4 and the specimen holders described on page 9 of Ref. 3.

Table III. Test Matrix[a]

Test	Specimen Sequence (from Bottom to Top of Test Column)[b]	Test Period, h	Test Temp.,°C
DC2	D9-R450-HT9-U5Fs-316SS-R450-S-U10Zr-D9-R450-T91-R450-HT9	724	656[c]
DC3	D9-R450-HT9-U10Zr-316SS-R450-S-U10Zr-D9-R450-T91-R450-HT9	720	750
DC4	316SS-036-HT9-029-T91-R450-D9	300	757[c]
DC5	316SS-029-D9-036-304SS-S-316SS-036-HT9-029-T91	150	800
DC6	316SS-R450-304SS-R450-D9	150	800
DC7	316SS-R450-304SS-R450-D9	150	802[c]
DC8	316SS-U5Fs-T91-029-HT9-036-304SS	300	706[c]
DC9	304SS-036-316SS-029-D9-036-316SS	150	802[c]
DC10	304SS-036-316SS-029-D9-036-316SS	150	777[c]
DC11	T91-036-D9-036-HT9-029-T91	300	731[c]
DC12	D9-U10Zr-316SS-036-D9-029-304SS-036-D9	700	758[c]

[a]Nominal fuel compositions were as follows: EFL029, U-8Pu-10Zr; R450, U-15Pu-11Zr; and EFL036, U-19Pu-10Zr.

[b]Hyphens denote fuel/clad interfaces; "S" denotes a stainless steel spacer.

[c]Corrected as explained in the Appendix.

Compatibility couple tests DC2-DC6 utilized specimen holders of Croloy (2¼Cr-1Mo). This material provides the desired low coefficient of expansion and was used to advantage in the precedent diffusion tests on uranium fuels described in Ref. 3. However, in test DC3, which was run at 750°C, a massive reaction occurred between the Croloy holder and the U-Pu-Zr fuel material in the test column. In this case a small holder/column radial gap allowed contact between the fuel and Croloy at one or more points. Test DC2, which was run at 656°C, showed no evidence of interaction between the fuel and the Croloy holder even though column/holder contact was almost certain. From this test evidence, one can conclude that the onset-of-melting temperature for interfaces between Croloy and U-Pu-Zr fuels falls somewhere between 656°C and 750°C.

In compatibility test DC4, which was run at 757°C, two innovations were applied to prevent Croloy/fuel interaction: the Croloy specimen holder surfaces were oxidized prior to assembly and a 0.003-in. Type 316 stainless steel foil wrap was used to enclose the test column. However, oxygen from the Croloy surfaces may have created some interference in the fuel/cladding diffusion dynamics, as evidenced by irregular grain boundary features in some of the test interfaces and on some clad outer surfaces. In consequence, the use of oxidized components in future compatibility tests was deemed unacceptable.

Compatibility test DC5, which was run at 800°C, included a 0.006-in.-thick Type 316 stainless steel foil wrapping around the test column. Test DC6 included a 0.006-in.-thick molybdenum wrap. The published fuel/clad compatibility results given in Table II of Ref. 4 provided some indication that these foil wraps would provide protection at that temperature. However, substantial melting of the test column occurred in both tests. Optical metallography of the test sections provided some evidence that the melting may have initiated in the foil area or, at least, that the foil transmitted the melting condition along the column. As a result, the Croloy specimen holder was abandoned and the holder design described in Section II.C was adopted.

Previous compatibility testing work generally utilized sealed glass ampoules to protect the test couples from atmospheric contamination. A quick turnaround can be obtained by this approach. Tests DC2-DC4 in this series were enclosed by glass ampoules. However, the available ampoule sealing

equipment was inadequate for specimen holders of the current, larger size and provided unreliable seals. This was demonstrated by the presence of a small leak in the ampoule of DC2. Subsequently, the welded metal closure capsule approach, which is described in Section II.C of this report, was adopted with special steps to provide a "quick welding turnaround" method of encapsulation of the compatibility test vehicles.

C. Prior Published Results

The early breeder reactor metal fuel/clad compatibility work was done on uranium fuels, as published in Ref. 1 and in other reports. Subsequently, a series of compatibility experiments was done on U-Pu-Zr fuels with Fe-, Ni- and V-base cladding alloys. The results of those tests are reported in Ref. 4. Table IV lists the pertinent information on the onset-of-melting temperature, T_m, taken from page 340 of that reference. The U-10Zr data have been included for comparison purposes. T_m has been defined by the referenced authors as the temperature at which a liquid phase is formed in the diffusion layer.[a] From inspection of the T_m values, it is assumed that the published ±25°C tolerances are a result of running the compatibility tests in a series of 50°C increments, i.e., 700°C, 750°C, 800°C, and 850°C, except for the U-10Zr fuel.

D. Experimental Results

1. Optical Metallography

Sections taken from samples listed in the compatibility test matrix of Table III were evaluated by optical metallography for evidence of onset-of-melting in the fuel/clad interfaces. The results of these evaluations are compiled in Table V. In this case the fuel/clad interface is described as a reaction zone. Table V identifies a number of fuel/clad interfaces that were broken during handling and in some cases were observed to be broken in the specimen holder before disassembly. In general, the ferritic clad/fuel interfaces appeared to be particularly brittle and very careful handling was required to maintain column integrity for those specimens.

---

[a] In the present report the terms onset-of-melting and incipient melting are also used to describe T_m.

Table IV. Melting at Interface Between Fuel and Fe- and Ni-Base Alloys (Ref. 4)

Fuel Alloy (wt.%)	Clad	T_m, °C
U-16.6Pu-6.3Zr	304 SS	725±25
	Hastelloy-X	725±25
U-15Pu-10Zr	16-15-6[a]	825±25
	16-25-6[a]	<850
	304 SS	825±25
	Haynes 56	825±25
	Incoloy 800	775±25
	N-155	<850
	Hastelloy-X	725±25
U-18.5Pu-14.1Zr	16-15-6	835±15
	Haynes 56	825±25
	304 SS	825±25
	16-25-6	<850
	N-155	825±25
	Incoloy 800	825±25
	Hastelloy-X	725±25
U-10Zr	304 SS	835±15

[a]Timken 16Ni-15Cr-6Mo and 16Ni-25Cr-6Mo.

All of the test couples that remained intact after thermal testing were inspected at 275X (and in some cases 500X) magnification for the presence of reaction zone products in the fuel/clad interface. The examinations were generally done both in the as-polished condition and after chemical etching of the clad component. In some cases the samples were reviewed in the as-polished condition, but after holding in the glovebox for 2-7 days, to allow glovebox atmosphere etching to enhance visual features on the fuel side of the interface. Chemical etching of the fuel side of the sections did not materially enhance the reaction zone for easier evaluation of liquid phase formation.

Fuel/clad interfaces that exhibit typical diffusion band characteristics are shown for an austenitic stainless steel clad in Fig. 2 and a ferritic clad in Fig. 3. There is no evidence of liquid phase formation in these interfaces. The Zr-rich band on the fuel side of the interface, which has

Table V. IFR Compatibility Test: Reaction Zone Results

Reaction Zone	Fuel[a]	Test	Time, h	Temp., °C[b]	Condition	Additional Observations
			Type 304 Austenitic Stainless Steel Clad			
1	036	DC8	300	706	Not Melted	
2	029	DC12	700	758	Not Melted	
3	036	DC12	700	758	Not Melted	
4	036	DC10	150	777	Not Melted	
5	R450	DC7	150	802	Not Melted	
6	R450	DC7	150	802	Not Melted	
7	036	DC9	150	802	Melted	Gross melting[c]
			Type 316 Austenitic Stainless Steel Clad			
8[e]	R450	DC2-2	724	656	Not Melted	Leaking[d]
9[e]	U-5Fs	DC8	300	706	Not Melted	
10	036	DC4-1	300	757	Not Melted	Oxidation[f]
11	036	DC12	700	758	Not Melted	
12	029	DC10	150	777	Not Melted	
13	036	DC10	150	777	Not Melted	
14	036	DC10	150	777	Not Melted	
15	R450	DC7	150	802	Not Melted	
16	029	DC9	150	802	Melted	Gross melting[c]
17	036	DC9	150	802	Melted	Gross melting[c]
18	036	DC9	150	802	Melted	Gross melting[c]
			D9 Austenitic Stainless Steel Clad			
19	R450	DC2-1	724	656	Not Melted	Leaking[d]
20	R450	DC2-2	724	656	Not Melted	Leaking[d]
21	036	DC11	300	731	Not Melted	
22	R450	DC4-2	300	757	Not Melted	Oxidation[f]
23[e]	029	DC12	700	758	Melted	
24[e]	036	DC12	700	758	Melted	
25	U-10Zr(052)	DC12	700	758	Melted	
26	029	DC10	150	777	Melted	46-μm depth,[g] 58% width[h]
27	036	DC10	150	777	Melted	115-μm depth,[g] 45% width[h]
28	R450	DC7	150	802	Not Melted	
29	029	DC9	150	802	Melted	Gross melting[c]
30	036	DC9	150	802	Melted	Gross melting[c]

Table V. (Contd.)

Reaction Zone	Fuel[a]	Test	Time, h	Temp., °C[b]	Condition	Additional Observations
			HT-9 Ferritic Stainless Steel Clad			
31	R450	DC2-1	724	656	Not Melted	Leaking[d]
32	R450	DC2-2	724	656	Not Melted	Leaking[d]
33	029	DC8	300	706	Not Melted	
34	036	DC8	300	706	Not Melted	
35	029	DC11	300	731	Not Melted	
36[e]	036	DC11	300	731	Melted	Few-μm depth,[g] >60% width[h]
37[e]	029	DC4-1	300	757	Not Melted	No band visible; Oxidation[f]
38[e]	036	DC4-1	300	757	Melted	81-μm depth,[g] >80% width;[h] Oxidation[f]
			T91 Ferritic Stainless Steel Clad			
39[e]	R450	DC2-2	724	656	Not Melted	Leaking[d]
40[e]	R450	DC2-2	724	656	Not Melted	Leaking[d]
41[e]	U-5Fs	DC8	300	706	Not Melted	No band visible
42	029	DC8	300	706	Not Melted	
43[e]	029	DC11	300	731	Melted	Major melting[i]
44	036	DC11	300	731	Melted	Gross melting[c]
45[e]	R450	DC4-2	300	757	Not Melted	Oxidation[f]
46[e]	029	DC4-2	300	757	Melted	58-μm depth,[g] >50% width;[h] Oxidation[f]

[a]Fuel compositions were as follows: R450, U-15Pu-11Zr (D350); EFL-029, U-8Pu-10Zr; and EFL-036, U-19Pu-10Zr.

[b]Test temperatures were corrected as explained in the Appendix.

[c]Defined as melting over a majority of the fuel sample.

[d]I.e., a substantial amount of oxygen entered capsule.

[e]Interface broken during disassembly.

[f]I.e., a small amount of oxygen was present in the capsule from oxidized holder surfaces.

[g]Refers to the reaction depth into the combined fuel and cladding.

[h]Refers to the reaction width along the interface.

[i]Defined as melting over less than a majority of the fuel sample.

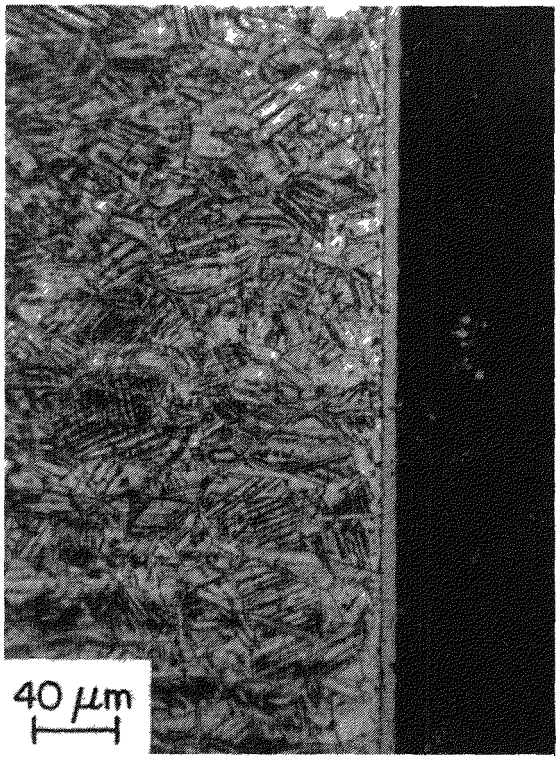

316 SS Clad R450 Fuel

Fig. 2. Typical Interface between Austenitic Stainless Steel Clad and U-15Pu-11Zr (R450) Fuel after 150 h at 802°C (Test DC7). No incipient melting is evident.

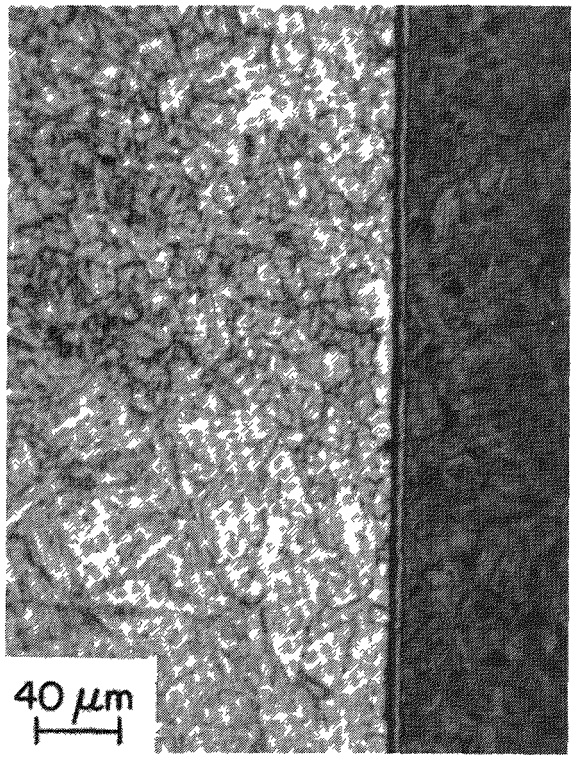

T91 Clad 029 Fuel

Fig. 3. Typical Interface between Ferritic Stainless Steel Clad and U-8Pu-10Zr (029) Fuel after 300 h at 706°C (Test DC8). No incipient melting is evident.

been reported in prior studies, is visible in these pictures. Figure 4 shows a characteristic zone of incipient melting in as-polished HT-9 clad, which had been in contact with U-19Pu-10Zr (EFL036) at 757°C for 300 h. In this case the fuel/clad interface broke during disassembly. On visual inspection, three distinct bands are seen in the reaction zone. These multiband features are commonly seen on the clad side of the regions that show incipient melting in the current tests. The banding feature has been further evaluated by SEM and the results are described in Section III.D.2 below.

Reaction zone formation had been interrupted at various stages of propagation in the current compatibility experiments. Figure 5 shows a liquid phase formation zone that could have been initiated shortly before

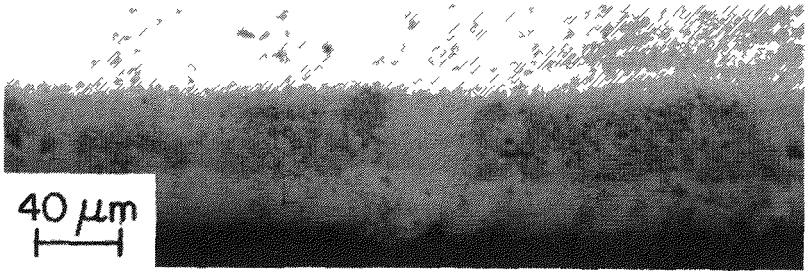

Fig. 4. Typical Zone of Incipient Melting. Interface between HT-9 (Ferritic Stainless Steel) Clad and U-19Pu-10Zr (036) Fuel after 300 h at 757°C (Test DC4).

test DC10 was ended. A substantial number of "early" incipient-melting zones have been found in these experiments in both austenitic and ferritic clad materials. This may indicate that incipient melting propagates very slowly, or may extinguish altogether, at temperatures just above the onset-of-melting temperature.

A number of the compatibility tests resulted in gross melting of the fuel and to a lesser extent the clad components. Some of these test sections were examined for clues to the reaction zone propagation rates in the gross melting state. From the visual examinations of DC9 and DC11, an assumption is made that at some time during the test, owing to other factors such as liquid phase volume, content of interstitials, and zirconium distribution in the fuel, the reaction zone formation rate accelerates substantially. In cases where entire fuel samples reached the molten state, the adjacent clad samples showed reaction zones generally covering fractional volumes.

There is some concern about the validity of multi-interface test results in cases where melting occurs in some of the interfaces but not in others. Visual evidence from the current tests indicates that massive melting of one sample in a test column may promote melting in adjacent samples, especially in the presence of wrapper foils or specimen holder surfaces that are in close proximity to the molten area. The interface melting results in those tests are deemed inconclusive. However, when incipient melting occurs in small areas or narrow bands, as exemplified by three molten zones in test DC12, it is evident that there is no effect on adjacent fuel/clad interfaces.

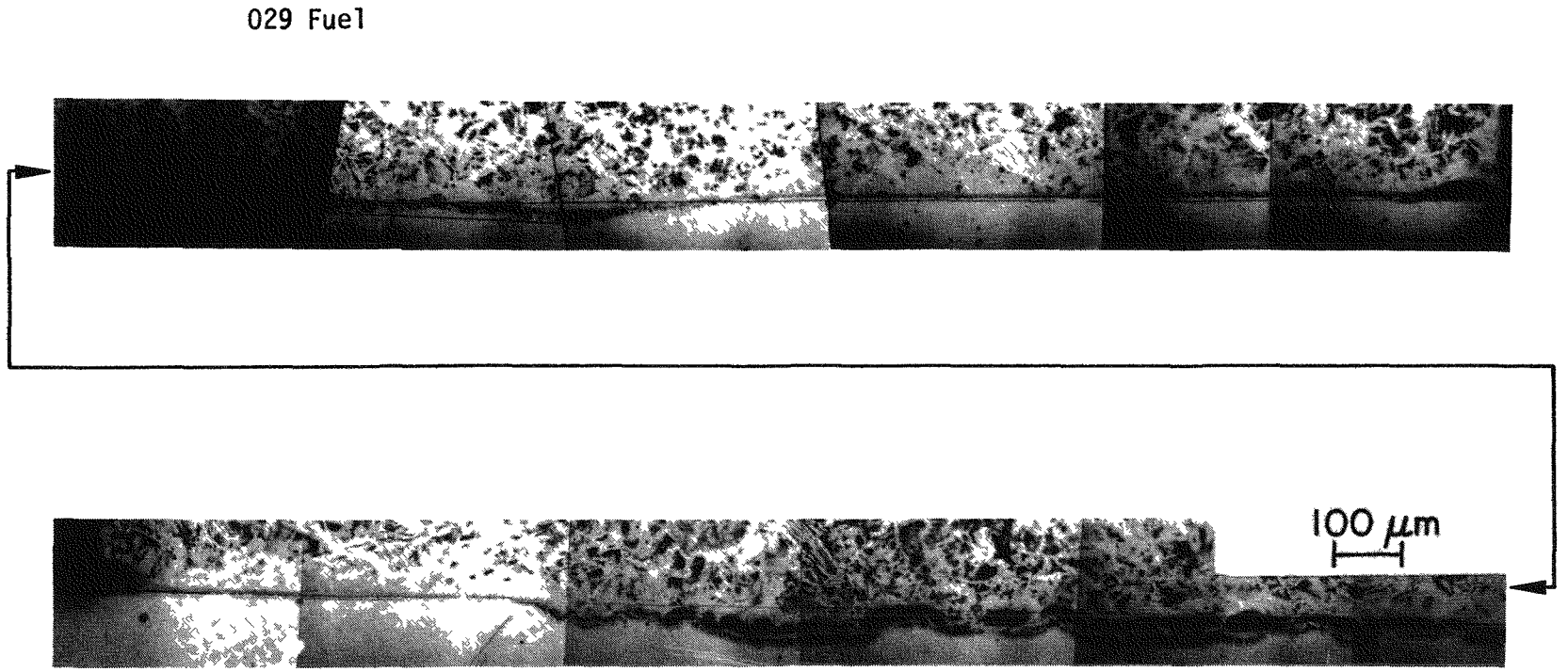

Fig. 5. Early Stage of Incipient Melting. Interface between D9 (Austenitic Stainless Steel) Clad and U-8Pu-10Zr (029) Fuel after 150 h at 777°C (Test DC10).

2. Scanning Electron Microscopy

In test DC4 (300 h at 757°C), the optical metallography clearly shows that significant fuel/clad interaction occurred in some of the fuel/clad couples. The high-plutonium fuel, EFL036, has formed an 80-μm, compound interaction zone with HT-9, whereas the lower plutonium fuel, EFL029, retains the narrow Zr-rich zone (Fig. 6) that also exists at 706°C (Fig. 7). In contrast, the T91 clad has formed a rather wide (maximum ∿50-μm) and irregular interaction zone with the low-plutonium fuel (Fig. 8). Both the 036/HT-9 and 029/T91 couples separated at the bulk-fuel interface during dismantling of the specimen holders.

The distribution of the major components in the interaction zone between HT-9 and EFL036 is shown in Fig. 9. The interaction zone consists of two major bands, i.e., an Fe- and Zr-rich band on the fuel side and a band consisting essentially of U-Pu and Fe on the clad side. This fuel-rich band is further divided into two structurally different sub-bands separated by an Fe-rich, narrow band of precipitates. The interaction zone between T91 and EFL029, shown enlarged in Fig. 10, has essentially the same zone structure, but without the band of precipitation. The partitioning of the compounds within the HT-9 interaction zone indicates that most of the zone was solid before the test was cooled to room temperature. It appears that the outermost band on the clad side was a U-Pu-Fe eutectic that moved in the direction of the clad during the test. Behind this molten band (Fig. 9) a complex multicomponent diffusion band continued to develop.

Test DC4 also contained an archive fuel sample, R450, with T91 and D9 clad interfaces. Neither of these clad materials showed an interaction zone with the R450 fuel. However, both developed a Zr-rich band (Fig. 11), similar to that found at the clad/fuel interface at 706°C (Fig. 7). No U-Pu-rich rim between the zirconium band and the clad was found in the R450 compatibility couples, as is described for DC8 at the top of Page 27 of this report.

Test DC8 shows no evidence of eutectic formation at any of the interfaces. Zirconium bands have formed on every interface, as shown in Fig. 7. These bands are somewhat irregular in width and the width varies from interface to interface. However, there appears to be no definite correlation between band width and either fuel batch or clad type. Only zirconium was detected in the zones. Further examination with the Auger microprobe

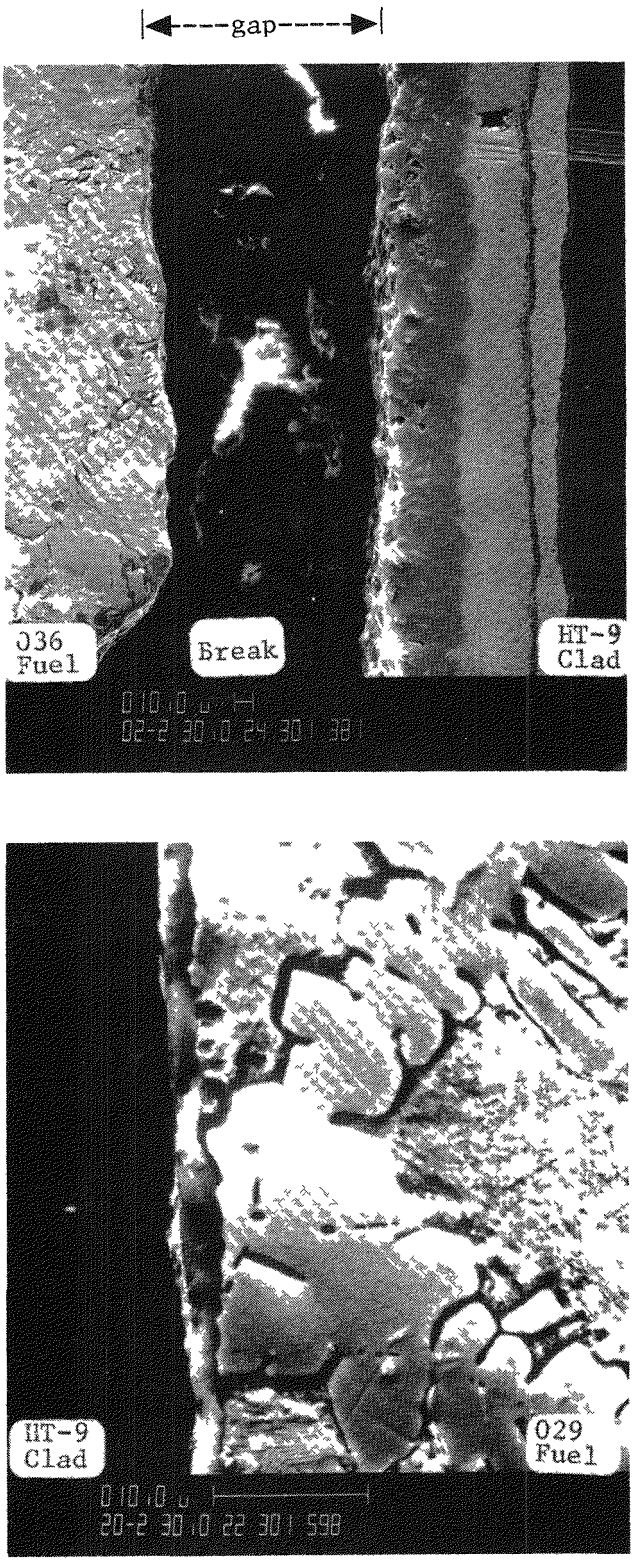

Fig. 6. Interaction Zones between HT-9 (Ferritic Stainless Steel) Clad and EFL Fuels after 300 h at 757°C (Test DC4).

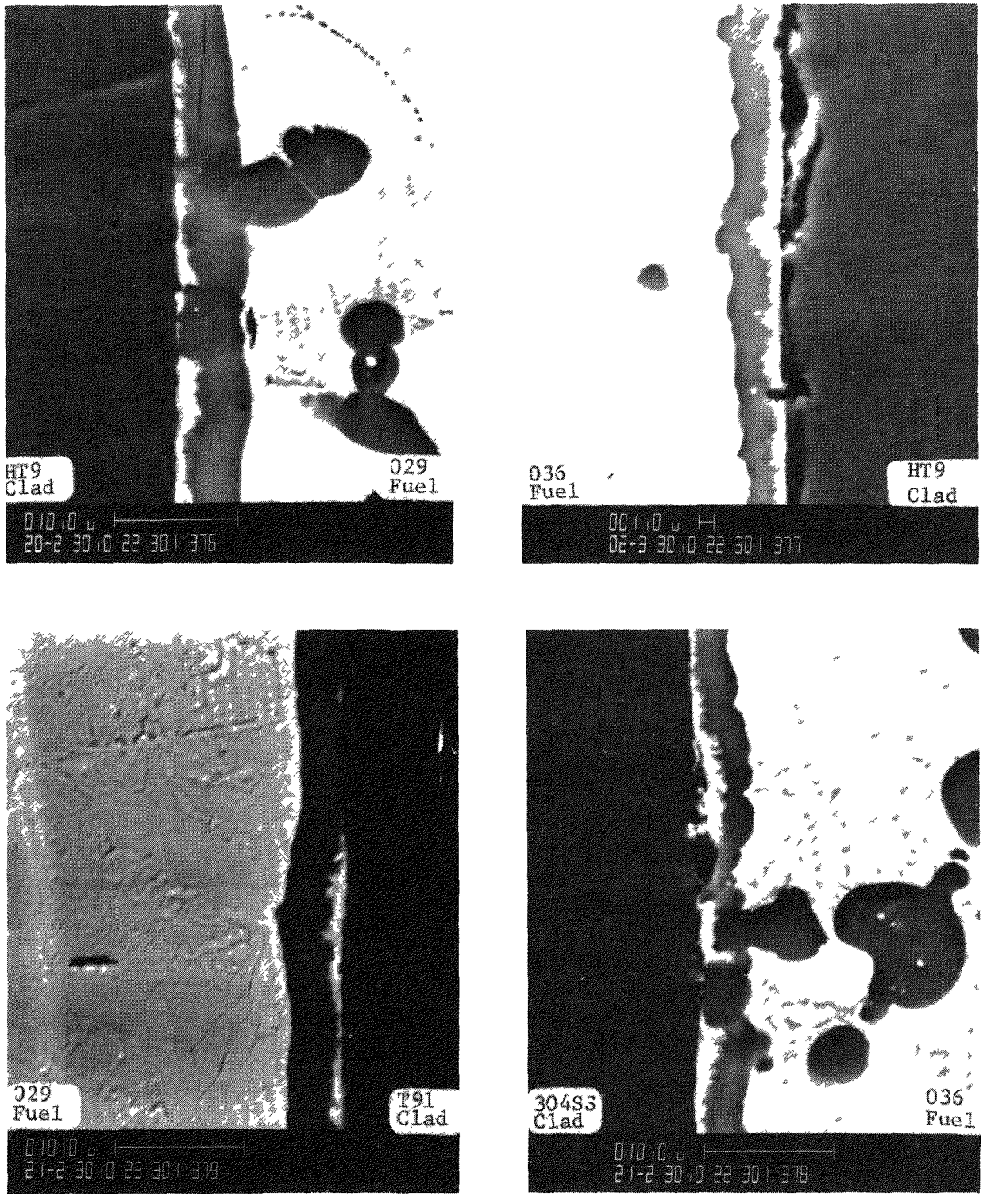

Fig. 7. Backscattered Electron Images of Interfaces between Various Clads and U-8Pu-10Zr (029) or U-19Pu-10Zr (036) Fuel after 300 h at 706°C (Test DC8).

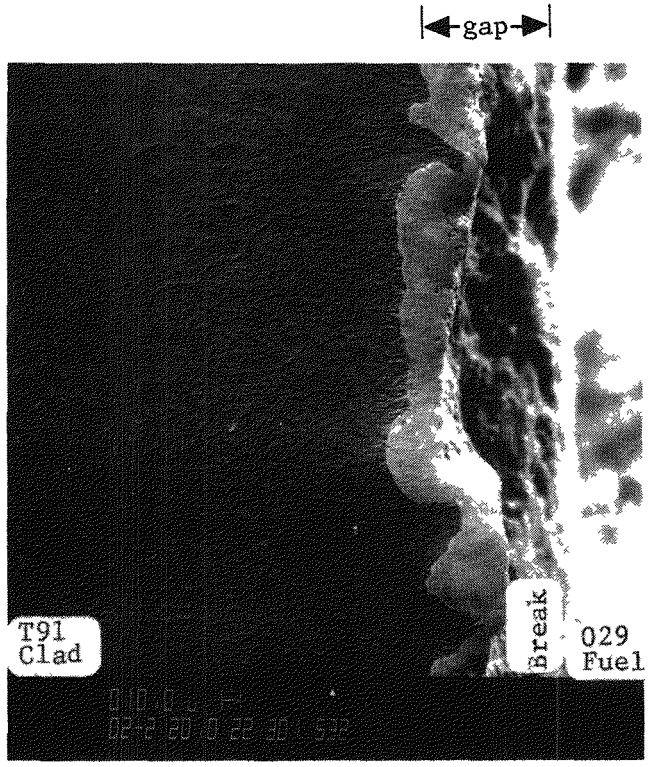

Fig. 8. Interaction Zone between T91 Clad and U-8Pu-10Zr (029) Fuel after 300 h at 757°C (Test DC4).

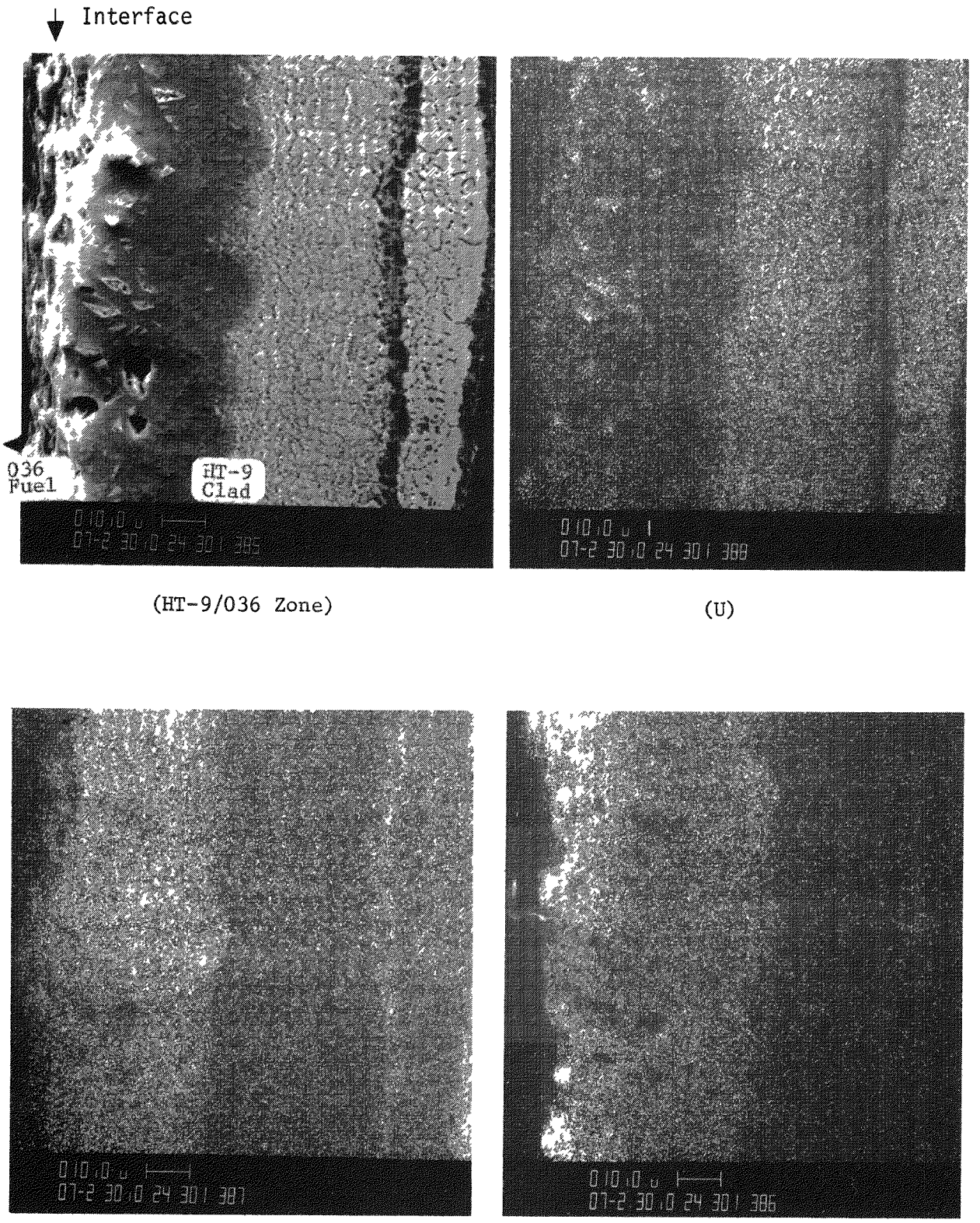

(HT-9/036 Zone) (U)

(Zr) (Fe)

Fig. 9. X-Ray Maps of Interaction Zone between HT-9 Clad and U-19Pu-10Zr (036) Fuel after 300 h at 757°C (Test DC4).

Fig. 10. Interaction Zone between T91 Clad and U-8Pu-10Zr (029) Fuel after 300 h at 757°C (Test DC4).

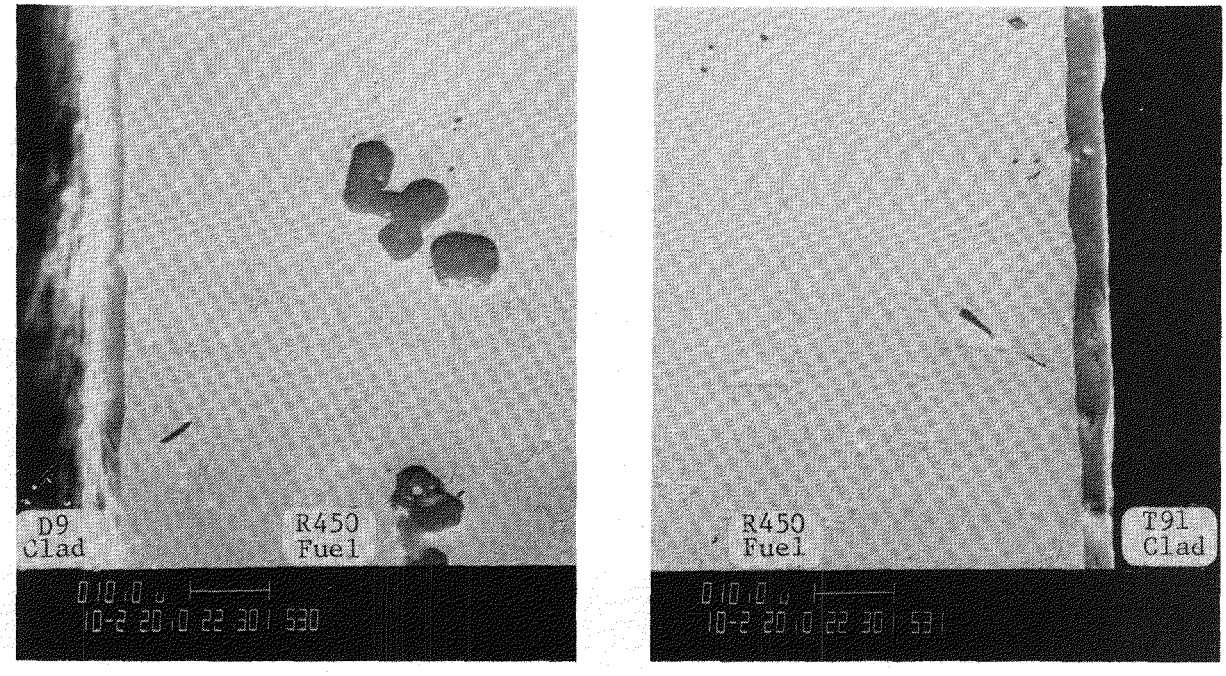

Fig. 11. Interfaces between U-15Pu-11Zr (R450) Archive Fuel and Clads after 300 h at 757°C (Test DC4).

will be required to determine whether oxygen, carbon, and/or nitrogen are present. These interstitial elements are suspected of playing a controlling role in the segregation of zirconium (Ref. 5).

Another common feature seen in DC8 is the very irregular band of fuel between the zirconium zone and the clad. This band contains uranium and plutonium in a much higher concentration than the bulk fuel. Some zirconium and iron are also present in this band.

IV. ANALYSIS AND DISCUSSION

A. Metallographic Results

The onset-of-melting test data presented in Section III of this report are summarized in Fig. 12. Temperatures at which liquid phase formation begins in the respective fuel/clad test couples may be tentatively identified from the data in Table V. The tentative melting points are placed midway between the highest non-melting temperature and the lowest melting temperature found for the respective fuel/clad interfaces. However, the T_m for R450 fuel test couples may be as high as 825°C, or even higher -- no tests were run above 802°C in the current series of experiments.

There is some question whether the ultimate onset-of-melting temperature can be determined in the type of short-term tests described here. Some probability exists that the complex diffusion mechanisms that occur with these multiphase materials may require longer test periods to generate equilibrium conditions for lowest-temperature liquid phase formation. However, the amount of disagreement between the current test results and an equilibrium T_m would be expected to be small, i.e., perhaps 25°C. The incipient-melting evidence uncovered in the latest experiment, DC12, suggests that a few additional 700- to 1000-h tests should be conducted in the areas where test data are sparse or results deviate somewhat from general patterns.

As described for Fig. 5, fuel/clad melting appears to begin at one or more points in the central portion of the interface. This could be the result of a lower Zr content in the fuel matrix at the central portion of the fuel casting. It is also frequently observed that the Zr-rich band on the fuel side of the interface is substantially thinner in the center. Another, unknown cause may be at work here. The reaction zone is expected to

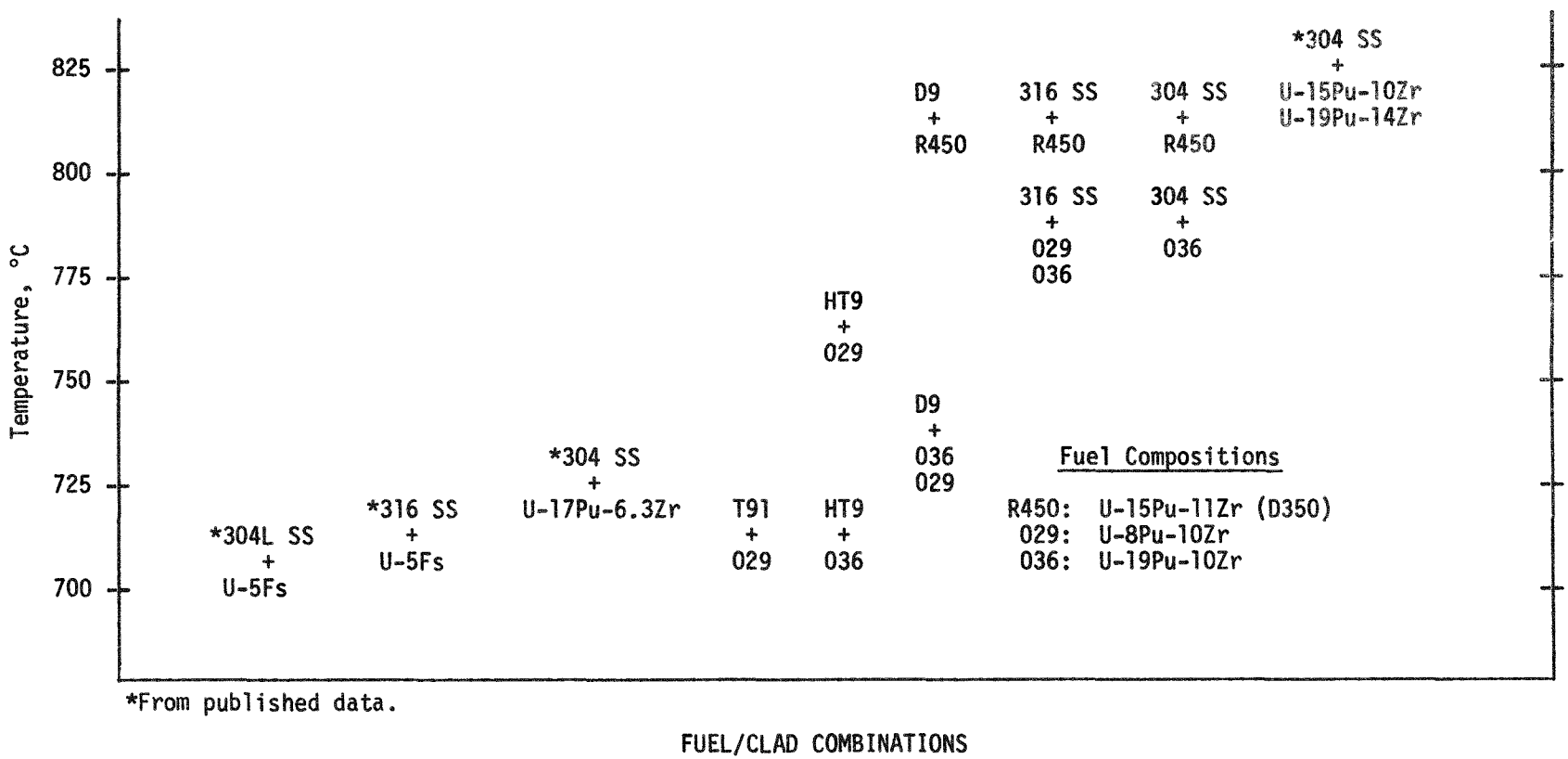

Fig. 12. Tentative Onset-of-Melting Points Deduced from Experimental Test Data.

propagate both along the interface and internally into the fuel and clad. However, the presence of voids, as seen in Fig. 5, at elevated temperature would tend to reduce the rate of melting propagation into the clad body by interrupting the path of atom diffusion across the interface. In all observed cases, the initial reaction zone appears to propagate more heavily into the clad, leaving a somewhat convex-shaped interfacial geometry when viewed from the clad side.

Figure 12 shows that R450, the U-Pu-Zr fuel manufactured by the Plutonium Fabrication Group in Building 350 in 1967, yields a somewhat higher incipient-melting point in austenitic stainless steel couples than the melting point produced with EFL fuels made in the ANL-West facility in 1985. The difference in incipient-melting point for the two fuels is about 25°C, except that the D9 clad compatibility couples appear to show a difference of more than 25°C. Some of the evidence indicates that the D9 alloy produces lower T_m points with EFL fuels than do the other austenitic clads. The reason for the difference between the R450 and EFL fuels is currently unknown and will be the subject of further metallurgical and chemical studies. Possibilities were thought to include a lower Pu content in the R450 fuel than the 15.1 wt.% originally reported, or a change in the diffusion mechanism as a result of the low carbon concentration (60 ppm) that was originally reported. However, new plutonium analyses were obtained in October 1985, which indicate a Pu content of ∿15.6 wt.%. Concentrations of oxygen and nitrogen interstitials in R450 were reported to be 500 ppm and 490 ppm, respectively. The interstitials content of EFL fuels has not been determined. Studies are under way to determine whether off-normal performance can be optimized, i.e., to maximize the onset-of-melting temperature, by tailoring the interstitial content in the fuel and perhaps the clad material (Ref. 6).

The incipient-melting temperature for ferritic stainless steel clad has been found to be lower than the T_m for austenitic stainless steel, when coupled with comparable fuels. The difference in incipient-melting temperature between the two types of clad ranges from 25°C to 50°C. In the ferritic stainless steel alloys, the incipient-melting temperature is found to decrease as the chromium content decreases from 12 wt.% (HT-9 alloy) to 9 wt.% (T91 alloy). A T91 clad alloy combination with fuel having a high Pu content

could possibly initiate melting below 725°C. Further tests are needed to establish this point. Slow propagation of the incipient-melting band just above the onset-of-melting temperature in ferritic alloys appears to follow a mechanism metallographically similar to that found in austenitic alloys.

Some evidence has been developed to indicate that an increased plutonium content in the fuel reduces the fuel/clad onset-of-melting temperature. The HT-9 data in Fig. 12 suggest this trend. However, the T_m difference between 8 wt.% Pu and 19 wt.% Pu fuels may be less for most clad alloys than for the HT-9. More compatibility experiments will need to be conducted with both ferritic and austenitic clads to better define this trend.

B. Correlation with Prior Studies

The incipient-melting temperatures of all the fuel/clad compatibility tests reported here fall above the T_m found by past workers for the EBR-II fuel (U-5Fs) and clads (Types 304 and 316 stainless steel). Thus, the current experimental results are considered to be favorable in light of the successful performance of the present EBR-II fuel at high burnup levels.

Current incipient-melting results for combinations of R450 U-Pu-Zr fuel with Types 304 and 316 stainless steel clad are in general agreement with the T_m results found previously on similar fuel/clad couples. Incipient-melting results for the EFL fuels fall in a lower temperature range, as discussed in Section IV.A above.

During the course of these onset-of-melting studies, a number of phenomena have been observed that suggest further metallurgical inquiry. The observed traits include (1) variations in fuel structures between fuel lots after heat treatment, (2) variations in fuel structures within a fuel lot after heat treatment, (3) influence of external and internal oxygen on diffusion kinetics, (4) clad intergranular penetration trends, and (5) zirconium buffer layer variations in the fuel. Some of these factors will be further investigated during the upcoming long-term fuel/clad diffusion studies. The other metallurgical questions may be referred to the attention of other IFR workers.

It is of general interest that past workers have not successfully drawn a specific correlation between T_m results obtained in compatibility tests and clad wall interactions seen during in-reactor fuel element burnup experiments. In-reactor clad surface degradation is not easily related to time-at-

temperature compatibility tests. However, comparison of the current incipient-melting test results with the results from past compatibility tests on the proven EBR-II fuel/clad system leads to a favorable conclusion regarding feasibility of the proposed IFR fuel/clad system.

C. SEM Studies

Scanning electron microscopy has confirmed the incipient-melting nature of the bands seen by optical microscopy. The characteristics of the interaction zones will be studied in more detail by Auger analysis, which will provide information on distribution of the light elements O, N, and C. In addition, a more quantitative analysis of the diffusion profiles adjacent to the interaction bands will be pursued.

The SEM micrographs clearly detail the Zr-rich bands that form on the fuel side of most fuel/clad compatibility couples. The formation of the Zr bands may be crucial to limit the development of further fuel/clad interactions and propagation of incipient-melting zones. It is possible that the Zr band did not develop in the earlier stages of the 757°C tests, except for the R450 fuel. A short preanneal at, say, 700°C may very well alter the interaction between HT-9 and T91 clads and the EFL fuels. The formation of Zr-rich bands probably involves fast-diffusing elements such as O, C, and/or N. Oxygen was considered to play a major role in Zr band formation in the work reported on Page 722 of Ref. 5. Auger analysis will be carried out in order to explore this seemingly important phenomenon.

V. CONCLUSIONS

1. No unexpected or restrictive fuel/clad eutectic-type formation events, or other chemical interaction events, were found in the compatibility tests on fuel and clad materials within the temperature range of the experiments.
2. U-Pu-Zr fuels are compatible with austenitic and ferritic stainless steel clad alloys to temperatures that are higher, except perhaps in the case of T91, than the measured onset-of-melting temperature for the EBR-II fuel/clad system in current use.

3. Onset-of-melting temperatures for the austenitic clad alloys are higher, by up to 50°C, than the melting temperatures for the ferritic stainless steel clad alloys. An exception is the D9 austenitic stainless steel combination with EFL fuels, which produces a lower T_m than the T_m from comparable couples with Types 304 and 316 stainless steel.
4. Onset-of-melting temperatures in couples between austenitic stainless steel clad alloys and archive (R450) fuel are higher by at least 25°C than those of similar couples with EFL fuels.
5. The HT-9 clad alloy test results, in particular, indicate that the percentage of plutonium in the fuel exerts some influence on the incipient-melting temperature.
6. The results of these experiments have raised other metallurgical questions related to fuel/clad interactions, which should be addressed in future studies.

ACKNOWLEDGMENTS

The author wishes to thank G. J. Talaber for doing the glovebox work on the compatibility experiments. D. R. Schmitt provided general glovebox and operational supervision during the course of these studies. The efforts of G. L. Hofman on SEM examination and analysis of compatibility couple interfaces are appreciated. H. R. Thresh has provided many valuable insights and general guidance to the overall program. Many helpful compatibility test discussions were held with D. L. Porter and E. L. Wood. Preliminary metallographic evaluations on as-received materials were performed by C. Steves and J. A. Zic.

REFERENCES

1. C. M. Walter, Interdiffusion Between Uranium-5 w/o Fissium Alloy and Type 304 Stainless Steel, Argonne National Laboratory Report ANL-6816 (March 1964).
2. S. T. Zegler, H. V. Rhude, Jr., and J. A. Lahti, Compatibility of Uranium-5 w/o Fissium Alloy with Types 304L and 316 Stainless Steel, Argonne National Laboratory Report ANL-7596 (Sept. 1969).
3. E. L. Wood and D. L. Porter, Fuel/Cladding Compatibility of U-10Zr and U-5Fs Fuels with Advanced Alloy Cladding Materials, Argonne National Laboratory Report ANL-IFR-13 (May 1985).
4. S. T. Zegler and C. M. Walter, "Compatibility Between Metallic U-Pu-Base Fuels and Potential Cladding Materials," AIME Symposium on Nuclear Fuels Technology, Nuclear Metallurgy 13, 335-344 (October 1967).
5. D. R. O'Boyle and A. E. Dwight, "The Uranium-Plutonium-Zirconium Ternary Alloy System," Plutonium 1970 and Other Actinides, Nuclear Metallurgy 17, Part II, 720-732 (1970).
6. H. R. Thresh, Concepts on the Potential for IFR Fuel/Clad Performance Enhancement, Argonne National Laboratory Technical Memorandum 8407-HRT-027 (Feb. 3, 1986).

APPENDIX: COMPATIBILITY TEST FURNACE TEMPERATURE CALIBRATIONS

A. Test Temperature Calibration Summary

The corrected test temperatures and the temperature uncertainties were calculated from calibrations done in October 1985 on the furnace equipment used in the compatibility experiments. Tabulated below are the values for corrected temperature and uncertainty that were calculated as described in Sections B and C below.

Compatibility Test	Goal Test Temp, °C	Corrected Temp., °C	Calculated Temp. Uncertainty, ±°C
DC12	750	758	5
DC11	725	731	5
DC10	775	777	5
DC9	800	802	5
DC8	700	706	5
DC7	800	802	5
DC4	750	757	6
DC2	650	656	9

B. Equipment Performance Specifications

1. National Bureau of Standards (NBS) type "S" thermocouple (NBS Test 225537). Based on the IPTS-68 Thermocouple Reference Tables, temperature correction is +1.0°C from 550°C to 700°C and +1.5°C from 725°C to 850°C. Uncertainty of the value is less than 0.5°C over the range, according to NBS.
2. Wahl Thermocouple Calibration Standard Instrument, model C-65. For type "S" thermocouples, the overall accuracy in 1 year is ±1.1°C, according to the manufacturer's specifications. The calibration accuracy (when used as a comparator) is ±0.5°C. The temperature scale resolution is ±0.5°C.
3. Fluke #2 temperature recording instrument. This instrument was used in conjunction with the Wahl unit and the accuracy is thereby equivalent, as demonstrated in operations log book entries. The temperature scale resolution is ±1/4°C.

C. Calibration Method Used to Determine Temperature Correction and Uncertainty Values

1. The NBS standard thermocouple temperature correction is +1.0°C from 550°C to 700°C and +1.5°C from 725°C to 850°C. Uncertainty of the value is ±0.5°C.
2. A working type "S" thermocouple, TC1, was calibrated against the NBS secondary standard. From the calibration results, the correction for TC1 vs the NBS secondary standard is +1.0°C from 550°C to 600°C and +1.5°C from 625°C to 850°C. Uncertainty of the TC1 temperature values includes ±0.5°C from the Wahl comparator mode and another ±0.5°C from the Wahl scale resolution factor.
3. Thermocouple TC1 was inserted into the furnace glovebox to calibrate recording thermocouples for furnaces #16 and #18. This was done after heat treatment run DC12 was completed. All lead wires were confirmed to be type "S" and junction blocks were checked for uniform temperature connections.
   a. Furnace #16 contains recording thermocouple CT1. Temperature trials were run between 650°C and 850°C in seven increments using the standard nickel heat sink, which has a temperature sensor well in the sink wall. Temperatures were recorded on both the Wahl instrument and the Fluke unit. Measurement corrections from TC1 and corresponding uncertainties were determined as follows:

Recorder	TC1-CT1, ΔT°C	TC1-CT1 Range, ΔT°C	Uncertainty, °C
Wahl	+7.0	5-9	±2
Fluke 2	+9.4	8-11.5	±2

   b. Furnace #18 contains recording thermocouple CT4. The same trials were run on Furnace 18 as described in 3a. above. Measurement corrections from TC1 and the corresponding uncertainties were determined as follows:

Recorder	TC1-CT4 ΔT°C	TC1-CT4 Range, ΔT°C	Uncertainty, °C
Wahl	+3.4	2-4.5	±1
Fluke	+6.3	4.5-7.5	±2

Additional uncertainties for these temperature values are obtained from the manufacturer's specifications as follows: ±1.1°C for Wahl drift and ±0.5°C for Wahl scale resolution.

4. Nickel heat sink cavity temperature calibration was done in a new sink that contained two adjacent thermocouple wells. A prototypic test capsule was made that allowed the temperature to be measured at the exact location of the test fuel column top. Measurements at the bottom of the heat sink cavity were assumed to duplicate the temperature measurement of the test fuel column bottom. Heat sink cavity temperatures were measured at 650°C and again at 850°C. Results were:[a]

Sink Well Temp, °C	Fuel Column Top, °C	Fuel Column Bottom, °C	Temperature Correction, °C
649	647	644	-4
849	846	843	-4

Temperature correction measurement uncertainties were assigned as follows: ±2°C for column temperature variation in the temperature range.

5. An inspection of the furnace run log books reveals that the test temperature was maintained within 2°C of the goal except for DC2, where the temperature varied by ±8°C. The uncertainty for run temperature has been very conservatively estimated at ±2.0°C, except that ±8°C has been used for DC2.
6. The furnace recording thermocouple temperature drift over the 9-month period of the compatibility experiments prior to this calibration run was estimated by a review of the furnace controller settings for the various experiments. Any recording thermocouple drift should be reflected in systematic change in the controller settings with time. A tabulation of the furnace controller settings is shown below:

[a]These results were obtained by a second heat sink test using thermocouple TC2, which was calibrated in the same manner as was TC1.

Test No.	Test Goal Temp, °C	Controller Setting, °C	Adjusted Control Temp, °C	Disagreement, °C
		Furnace #16		
DC4	750	717	720	3
DC8	700	671	670	1
DC11	725	694/695	695	1
DC12	750	719/721	720	Ref
		Furnace #18		
DC7	800	775/776	777	1-2
DC9	800	775/776	777	1-2
DC10	775	751/753	752	Ref

From this tabulation, it can be concluded that the 9-month recording thermocouple temperature drift is very likely less than ±4°C for test DC4 and ±2°C for all other tests. The ±2°C drift uncertainty includes test DC2, which was run with recording thermocouple CT1, but which used an old controller.

7. A calculation example for temperature correction on test DC12 is given below.

Temperature correction = C.1. + C.2. + C.3. + C.4.

= +1.5 + 1.5 + 9.4 + (-4)

= +8.4°C.

where: C.1. refers to NBS standard thermocouple values.

C.2. refers to "S" type working thermocouple values.

C.3. refers to furnace #16 recording thermocouple values.

C.4. refers to heat sink fuel column values.

C.5. refers to test temperature uncertainty.

C.6. refers to recording thermocouple drift uncertainty.

The measurement uncertainty for DC12 is calculated as follows:

$$\text{Measurement uncertainty} = \sqrt{C.1. + C.2. + C.3. + C.4. + C.5. + C.6.}$$

$$= 0.5^2 + (0.5^2 + 0.5^2) + (2.0^2 + 1.1^2 + 0.5^2) + (2.0^2 + 0.5^2 + 0.5^2) + 2.0^2 + 2.0^2$$

$$= \pm 4.3°C.$$

This result is a reasonable uncertainty for this type of test. It can now be said that the DC12 run temperature was 758 ±5°C.